ISSN: 2588-4115; Infection Epidemiology and Microbiology. 2025;11(1):63-75 10.52547/iem.11.1.63

Biosynthesis of Copper Nanoparticles using Artemisia biennis Willd Plant Extract for Antibacterial and Anti-Biofilm Activities

ARTICLE INFO

Article Type
Original Article

Authors
Sadaf Fazeli, *MSc*[1]
Fatemeh Rafiee, *PhD*[1*]
Atousa Ferdousi. *PhD*[1]

[1] Department of Microbiology, Shahr-e-Qods Branch, Islamic Azad University, Tehran, Iran

*** *Correspondence***
Department of Microbiology, Shahr-e-Qods Branch, Islamic Azad University, Tehran, Iran.
E-mail: Rafiee_ar@qodsiau.ac.ir

How to cite this article
Fazeli S., Rafiee F., Ferdousi A. Biosynthesis of Copper Nanoparticles using Artemisia biennis Willd Plant Extract for Antibacterial and Anti-Biofilm Activities. Infection Epidemiology and Microbiology. 2025;11(1): 63-75.

Article History
Received: June 25, 2024
Accepted: December 16, 2024
Published: February 22, 2025

ABSTRACT

Background: This research aimed to assess the antibacterial and anti-biofilm properties of copper nanoparticles (CuNPs) produced using *Artemisia biennis* Willd through an eco-friendly approach, targeting four pathogenic bacteria.

Materials & Methods: *A. biennis* Willd extract with unit numbers "15.62-125" was prepared through maceration, drying, and powdering. Particle size distribution (PSD), dynamic light scattering (DLS), zeta potential, X-ray diffraction (XRD), and Fourier-transform infrared spectroscopy (FT-IR) tests were used to characterize the synthesized CuNPs. Minimum inhibitory concentrations (MICs), minimum bactericidal concentrations (MBCs), and sub-minimum inhibitory concentrations (sub-MICs) were determined to investigate the antibacterial and anti-biofilm activities of CuNPs against *Staphylococcus aureus* ATCC 25923, *Enterococcus faecalis* ATCC 29212, *Escherichia coli* ATCC 25922, and *Klebsiella pneumoniae* ATCC 13883.

Findings: CuNPs synthesized using *A. biennis* Willd extract exhibited a brown color change with particle sizes mainly 30-40 nm by PSD. DLS indicated uniform distribution and hydrodynamic synthesis of particles with a zeta potential of -37.8. XRD and FTIR confirmed copper nanoparticle biosynthesis. The MICs of CuNPs were 15.62-62.5 µg/mL, with *S. aureus* and *K. pneumonia* revealing the highest and lowest antimicrobial drug resistance, respectively. This trend was repeated for MBCs and sub-MICs, ranging from 15.62-125 and 7.8-31.25 µg/mL, respectively. Bacterial strains were unable to form biofilms at sub-MICs. The anti-biofilm effects of CuNPs were more significant on Gram-negative bacteria.

Conclusion: CuNPs synthesized using *A. biennis* Willd extract by a green method show promising anti-biofilm and antibacterial characteristics against bacteria, suggesting their potential for treating bacterial infections.

Keywords: *Artemisia biennis* Willd, Copper nanoparticles, Green synthesis, Antimicrobial drug resistance, Anti-biofilm

CITATION LINKS

[1] Sabzi S, et al. Genome-wide... [2] Shahbazi S, et al. Identification of... [3] Shahkolahi S, et al. Detection of ESBL... [4] Taati Moghadam M. The evaluation of... [5] Lewis K. New approaches to... [6] Rahmati F. Identification and... [7] Magalhães C. To give or not to... [8] Shahbazi S, et al. In silico and in... [9] Reygaert WC. An overview... [10] Rahmati F. Characterization of... [11] Shahbazi S. Zinc oxide nanoparticles... [12] Shivaee A. Prevalence of ... [13] Moghadam MT. Helicobacter pylori... [14] Rahmati F. New insights... [15] Ruhal R, Kataria R. Biofilm patterns in... [16] Rahmati F. Microencapsulation ... [17] Shahbazi S. Design and... [18] Sabzi S. Polydopamine-based... [19] Parvaei M, Habibi M. Immunostimulatory... [20] Rahmati F. Impact of... [21] Jayarambabu N. Green synthesis of... [22] Wang C. et al. In situ synthesis... [23] Zhou X. Reactive oxygenated... [24] Fan X, Yahia LH, Sacher E. Antimicrobial... [25] Ameen F. Optimization of... [26] Ying S, et al. Green synthesis... [27] Hussain M, et al. Traditional uses... [28] Sancar PY. The molecular... [29] Tambun R. Performance... [30] De Sousa ES. Factors influencing... [31] Suresh S, et al. Green synthesis... [32] El-Seedi HR, El-Shabasy RM, et al. Metal... [33] Yadav S. Biogenic synthesis... [34] Vijayaraghavan K. Plant-mediated... [35] Gulati S. Capping agents... [36] El-Rab SM. Green synthesis... [37] Ijaz I. Detail review... [38] Dikshit PK, et al. Green synthesis ... [39] Al-Khafaji MA. Green synthesis... [40] Karimi B. Green synthesis... [41] Hayat K. Green synthesized... [42] Rajeshkumar S, et al. Antibacterial and... [43] Saranyaadevi K. Synthesis... [44] Rajesh K. Assisted green... [45] Valdez-Salas B, et al. Structure-activity... [46] Barchiesi D, et al. Performance of... [47] Amjad R, et al. Green synthesis... [48] Ismail M. Green synthesis... [49] Ghosh MK. Green synthesis... [50] Mali SC. Green synthesis... [51] Sacoto-Figueroa FK, et al. Molecular... [52] Ullah H, Wilfred CD, Shaharun MS. Green... [53] Pandit R, Gaikwad S, Rai M. Biogenic... [54] Müller E, Behra R, Sigg L. Toxicity of... [55] Mali SC, Raj S, Trivedi R. Biosynthesis of... [56] Shende S. Green synthesis... [57] Shanmugapriya J, et al. Green synthesis of... [58] Ahmad T. Effect of... [59] Bhavyasree P. Green synthesised... [60] Khorsandi K. A mechanistic perspective... [61] Govarthanan M, et al. Cottonseed... [62] Kumar PV. Green synthesis... [63] Nisar P. Antimicrobial... [64] Kaviya S. Biosynthesis... [65] Tovar-Corona A. Green synthesis... [66] Eshed M. A Zn-doped CuO... [67] Ghasemian E. Evaluating the... [68] Shamshad S. Current trends...

Introduction

During the past decades, antimicrobial drug resistance has been one of the most problematic issues for humans in biomedical sectors [1, 2]. The occurrence of infectious diseases like urinary tract infections (UTIs) and septicemia results in extended hospital stays, increased referrals to specialists, prolonged recovery periods, and elevated health care expenses [3, 4]. The majority of studies conducted over the last half century have focused on exploring promising antibacterial components with bactericidal or bacteriostatic properties [5]. The main issue that causes antimicrobial drug resistance is the selective pressure, which occurs when not all bacteria are susceptible to the antibiotic used to treat the infection, and the surviving bacteria could continue to multiply [6]. Selection pressure is a natural phenomenon that could be mitigated but not completely eliminated. Indiscriminate use of antibiotics is effective in increasing the rate of selective pressure [7]. Acquired antimicrobial drug resistance indicates a real alteration in the genetic makeup of a bacterium, resulting in a situation where a medication that was previously effective against living organisms is no longer effective [8, 9]. Compared to Gram-positive bacteria, most Gram-negative bacteria show more antimicrobial drug resistance due to the presence of an outer membrane and facilitating the presence of beta-lactamase enzymes encoded by plasmids as fragments of bacterial DNA [10, 11]. Biofilm could be considered as another strategy that some microorganisms, including bacteria, fungi, and algae, use to protect themselves from harmful effects and forces in the natural environment. Biofilm is the accumulation of microorganism cells, which is formed on various surfaces such as catheters, ventilators, and patients' wounds and is covered by extracellular polymeric materials [12, 13]. Many bacteria could form biofilms, which could cause chronic infections such as endocardial, wound, and lung epithelial infections, especially in patients with cystic fibrosis, persistent inflammation, and tissue damage due to their high antimicrobial drug resistance [14, 15].

Nanoparticles (NPs) are clusters of atoms ranging in size from 1 to 100 nanometers, which exhibit variations in their physical, optical, thermal, chemical, electrical, mechanical, and biological characteristics compared to their natural dimensions [16]. Also, normal-sized elements/components have small surface-to-volume ratios, slow dissolution, and difficulty in uptake into cells [17-19]. The characteristics of NPs are influenced by various factors, including their surface properties, shape, composition, size distribution, and any coatings they may have [20]. Based on the published literature, metal NPs like copper (Cu) are recognized as promising NPs with antibacterial properties [21, 22]. CuNPs have some unique properties such as small particle size, high surface-to-volume ratio, biocompatibility, and high biological and chemical reactivity, which help effectively kill bacterial cells [23]. CuNPs affect the cell membrane due to their affinity for amines and carboxyl groups on bacterial cell surfaces, and after entering the cell, they bind to DNA molecules and disrupt helical structures by producing reactive oxygen species (ROS); thus, they disrupt the cell membrane and cause direct cytotoxicity [24, 25]. The production of NPs by green synthesis method, which is environmentally friendly and plant-based, is widely used in nanoscience. This method does not require high pressure, energy, and temperature as well as toxic chemicals. Also, it is more uniform than other methods in terms of NP size distribution and stability [26]. The genus *Artemisia* is a diverse and widely-distributed group of plants found globally. *Artemisia* species could be found as perennial, biennial, or annual herbs as well

as small shrubs [27]. *A. biennis* Willd is known to contain various chemical compounds, including monoterpenes, sesquiterpenes, sesquiterpene lactones, flavonoids, coumarins, sterols, and polyacetylenes [28]. This plant exhibits several biological activities, such as cytotoxic and anti-inflammatory effects.

Objectives: For the first time, this study aimed to evaluate the antibacterial and anti-biofilm effects of CuNPs produced by green synthesis method using *A. biennis* Willd extract against Staphylococcus aureus ATCC 25923, *Enterococcus faecalis* ATCC 29212, *Escherichia coli* ATCC 25922, and *Klebsiella pneumoniae* ATCC 13883.

Materials and Methods

Preparation of *A. biennis* Willd extract and synthesis of CuNPs: *A. biennis* Willd was purchased from the Bank of Iranian Biological Reserve Center (Herbarium number 1328). The plant was then dried in a dark place to be completely powdered by grinding. Then 10 g of the obtained powder was added to 50 mL of water, and its aqueous extract was prepared by maceration method [29] and passed through a filter paper (Sigma-Aldrich Co, USA).

For the green synthesis of CuNPs using the extract, 200 mL of copper nitrate solution (0.01 M) was mixed with 8 mL of aqueous extract solution. The reaction was carried out at room temperature, and the color change was observed. The resulting dark solution was placed on a shaker (Thermos Fisher Scientific CO, USA) for two hours and then poured into falcon tubes and centrifuged (Thermos Fisher Scientific CO, USA) at 9000 rpm for 30 min.

The supernatant (containing the extract compounds) was discarded, and the precipitate was washed with distilled water and centrifuged. Finally, the obtained CuNPs were dried in an incubator at 37 °C.

Investigating the characteristics of the synthesized CuNPs

Dynamic light scattering (DLS) analysis: This test was carried out with the standard procedure of DLS-Zeta (SZ-100 model, Horiba Co, Japan) to determine the particle size distribution (PSD) and zeta potential of CuNPs, showing the physical characteristics influencing the behavior of CuNPs in colloidal solutions. DLS works by irradiating light onto a sample, analyzing the intensities of the detected peaks, and assessing the speed of particle movement. The size of NPs plays a crucial role in the effective accumulate of drugs in the intended tissue, the efficiency of treatment, their ability to permeate into blood vessels, and the transport and stability of NPs.

X-ray diffraction (XRD) analysis: The XDR test was utilized to determine crystal structure parameters, including lattice constant and geometry, which characterize the quality of unknown substances, phases, crystal size, single crystal orientations, and lattice defects. For this purpose, a powder X-ray diffractometer (X-Pert Pro model, PA Nalytical Co, Netherland) was applied with a copper anode lamp source (wavelength: λ=1.5406A°).

Fourier-transform infrared spectroscopy: Ultimately, FT-IR (Spectrum two model, PerkinElmer Co, USA) was utilized to analyze the chemical bonds in the sample using the KBr pellet method. The spectra were recorded in the wavelength range of 500–4000 cm^{-1} with a resolution of 1 cm^{-1}. To analyze CuNPs, the powder was examined under a microscope while the energy of the laser photons was adjusted either upward or downward. This energy shift provided insights into the vibration modes present in the system.

Evaluation of the antimicrobial and anti-biofilm effects of CuNPs against bacteria: In this test, MICs (minimum inhibitory concentrations) and MBCs (minimum

bactericidal concentrations) were calculated against *S. aureus* ATCC 25923, *E. faecalis* ATCC 29212, *E. coli* ATCC 25922, and *K. pneumonia*. To determine MICs, 96-well plates (Sigma-Aldrich Co, USA), a concentration range of 7.8-140 µg/mL of CuNPs, 95 µL of Mueller Hinton broth medium (Sigma-Aldrich Co, USA), and 5 µL of microbial suspension (separately for each bacterium) were used according to the serial dilution method. Negative and positive controls were also considered. After keeping the microplates in an incubator (Thermos Fisher Scientific CO, USA) for 24 hrs at 37 ºC, optical densities (OD) were read at 620 nm by an ELISA reader (Shimadzu Co, Japan) for MICs, and lower concentrations were considered as sub-MICs. The MBCs of CuNPs were determined according to the CLSI standard [30] as follows. One loop of the dilution representing the MIC and one dilution before and after which were cultured on Mueller Hinton agar plates. After incubation, MBC was the first dilution at which no bacterial growth was observed. A fresh culture of bacterial isolates was inoculated in tryptic soy broth (TSB) medium (Merck Co, Germany) containing 2% glucose to obtain a bacterial suspension with a turbidity corresponding to 0.5 McFarland. Then 100 µL of bacterial suspension and 50 µL of CuNPs at sub-MICs were added to each well. After incubation at 37 °C for 24 hrs, the supernatants were removed, and the sediments were washed three times with sterile physiological serum. After drying the plates, biofilm quantification was done by adding 200 µL of 33% acetic acid to each well. Finally, OD at 570 nm was read with an ELISA (enzyme-linked immunosorbent assay) reader. Wells without bacteria were considered as negative controls, while those with bacterial suspensions were considered as positive controls similar to the previous test. To promote biofilm development, strains were grown on Congo red agar medium (Merck Co, Germany). Essentially, bacteria that do not produce biofilms could not form any black colonies on the agar.

Statistical analysis: Data were analyzed using SPSS statistical software Version 21.0. MIC, sub-MIC, and MBC values of CuNPs against the tested bacterial strains were assessed. Each experiment was conducted three times. To evaluate the significance of differences in MIC, sub-MIC, and MBC values, one-way analysis of variance (ANOVA) was applied, followed by Tukey's post-hoc test for antibacterial and anti-biofilm tests, their p-values are shown in Figure 5.

Findings

Synthesis of CuNPs using *A. biennis* Willd extract: The aqueous extract of *A. biennis* Willd was obtained through the maceration extraction technique (Figure 1). Then copper nitrate was utilized for the environmentally-friendly production of CuNPs, with the observed color change serving as an indication of successful CuNP biosynthesis (Figure 2). This experiment was repeated in three falcon tubes to ensure the test accuracy. All three falcon tubes contained *A. biennis* Willd aqueous extract solution and copper nitrate solution and were kept at room temperature to monitor the color change resulting from CuNP synthesis.

Characteristics of the synthesized CuNPs: As shown in Figure 3a, the graph depicting the PSD of the synthesized CuNPs revealed a single peak, suggesting that CuNPs were monodispersed in the analyzed sample. Also, 95% of the measured CuNPs were smaller than 100 nm. Additionally, their classification as NPs (with diameters under 100 nm) was confirmed. Figure 3b illustrates the synthesized CuNPs by the nucleation and growth mechanism with a spherical and quasi-spherical shape displaying a somewhat puffy appearance in certain areas. This structure is caused by chemical reduction

Figure 1) Aqueous extract of *A. biennis* Willd obtained using maceration method

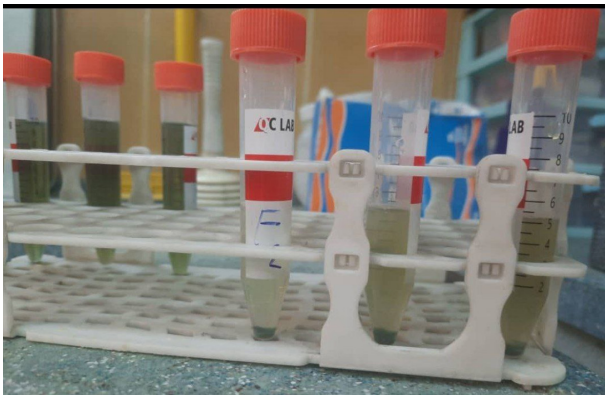

Figure 2) Production of CuNPs by green synthesis method

and swift aggregation of Cu^{+} ions. In this figure, the spheres are uniformly interconnected, creating a network with a lumpy texture in some regions. By assessing the diameter of 514 particles, the average diameter and standard deviation of CuNPs were found to be 41.92 and 16.92 nm, respectively. Moreover, the majority of CuNPs were in the size range of 30 to 40 nm, and the closeness of this range to the average particle size indicated a normal distribution of CuNP sizes. According to the findings presented in Figure 4a, the produced CuNPs were 182.5 nm in diameter, suggesting the successful hydrodynamic synthesis of nanoparticles. Additionally, the particle distribution index was recorded at 1.317, indicating a consistent size distribution of CuNPs. According to Figure 4b, these nanoparticles had a surface potential equal to -37.8 mV.

By comparing the diffraction pattern of the observed peaks with the reference diffraction patterns, it was determined that this sample corresponded to the following crystal phases (Figure 4c): 1) Cu crystalline phase with JCPDS reference code (No. 00-003-1018) and cubic crystal structure, 2) CuO phase with JCPDS reference code (No. 00-048-1548) and monoclinic crystal structure, 3) Cu_2O phase with JCPDS reference code (No. 00-005-0667) and cubic crystal structure, and 4) $CuCl_2$ phase with JCPDS reference code (No. 00-033-0451) and monoclinic crystal structure.

Afterwards some of the raw materials remained as $CuCl_2$, while others reverted to CuO, and some $CuCl_2$ was converted to Cu. Additionally, a broad peak was detected at an angle less than 10^0, which is typical in the green synthesis of nanoparticles and is attributed to the presence of organic groups with amorphous structures on the nanoparticles' surfaces, which contributes to their stabilization in the colloid. Using Scherer's relation, the crystal size of Cu, CuO, Cu_2O, and $CuCl_2$ nanoparticles was determined to be 5.08, 5.85, 5.22, and 14.4 nm, respectively [31].

Figure 4d shows the FTIR spectrum of the synthesized CuNPs.

The peaks at 3923, 3774, and 3427 cm^{-1} correspond to the stretching vibrations of O-H bonds in the phenols, terpenoids, and saponins present in *A. biennis* Willd extract as well as water molecules adsorbed on the surface of CuNPs [32]. Additionally, the peaks at 2924 and 2857 cm^{-1} are associated with the asymmetric and symmetric stretching vibrations of C-H bonds in methyl and methylene groups, respectively. The peak at 1620 cm^{-1} is linked to the stretching vibration of the C=O bond in the carbonyl group as well as the bending vibration of the O-H bond

or the stretching vibration of C=C bonds in the aromatic rings of the compounds found in the extract. Furthermore, the peak observed at 1428 cm^{-1} is associated with the bending vibrations of the C-H bond found in different compounds within this extract, while the peak at 1123 cm^{-1} corresponds to the stretching vibrations of carbon-oxygen bonds, including C-OH and C-O-C [33].

Ultimately, the peaks associated with the bending vibration of C-H bonds and the stretching vibration of Cu-O bonds in CuNPs are at 627 and 877 cm^{-1}, respectively. These findings show that the compounds derived from the extract act as a capping agent on the surface of CuNPs [34]. Capping agents are described as "binding molecules" utilized in small amounts during the production of NPs. These agents play a crucial role in the production of small-sized NPs and are commonly utilized in colloidal synthesis of NPs to prevent excessive growth [16, 35].

Determination of MICs, SubMICs, MBCs, and anti-biofilm properties of CuNPs: The findings indicated that the MICs of CuNPs ranged from 15.62 to 62.5 µg/mL (Table 1), with *S. aureus* and *K. pneumonia* exhibiting the highest and lowest antimicrobial drug re-

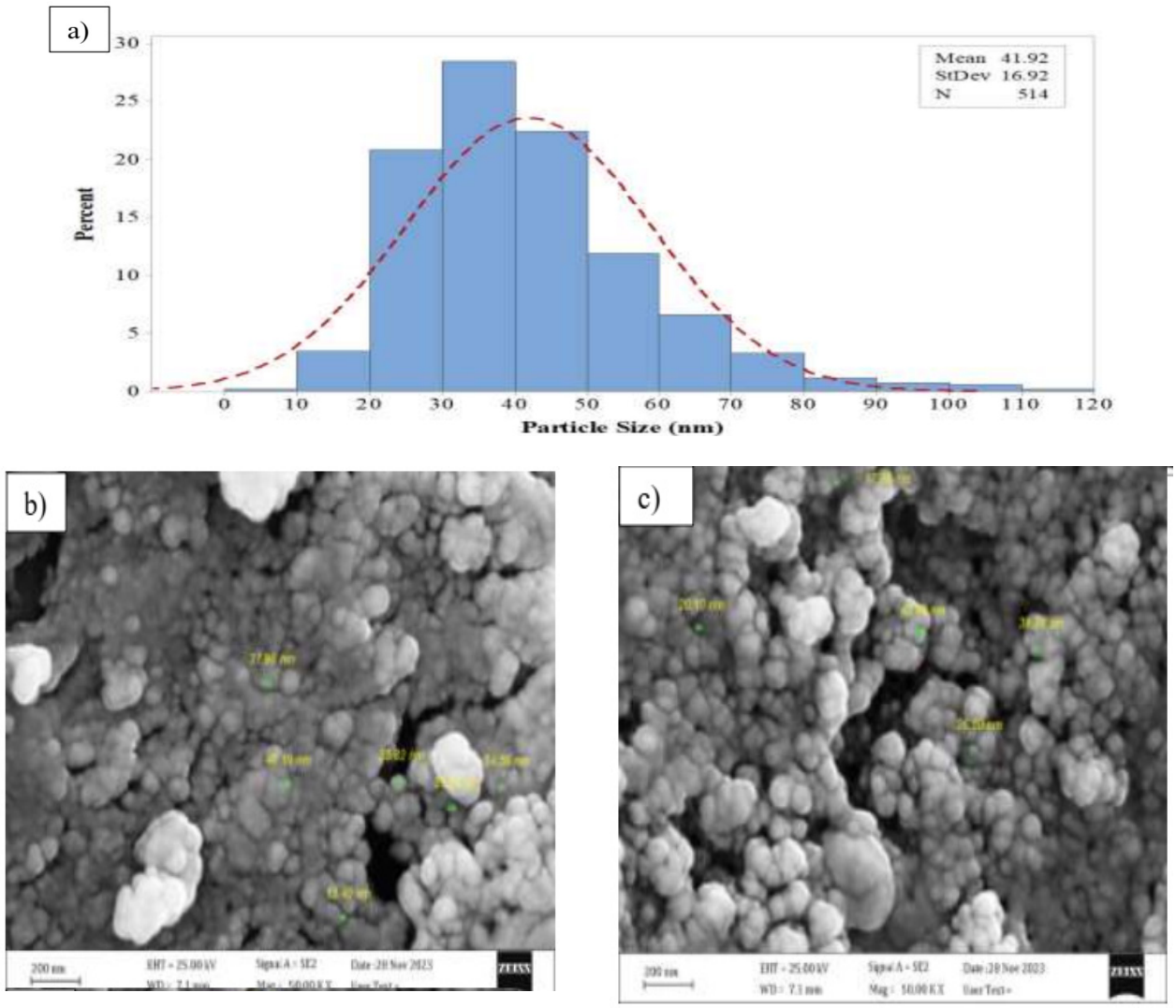

Figure 3) a) PSD test results of CuNPs produced by green synthesis method. PSD revealed a single peak, suggesting that CuNPs were monodispersed in the analyzed sample, b) shape and size of CuNPs by PSD test at 200 and c) 100 nm magnifications

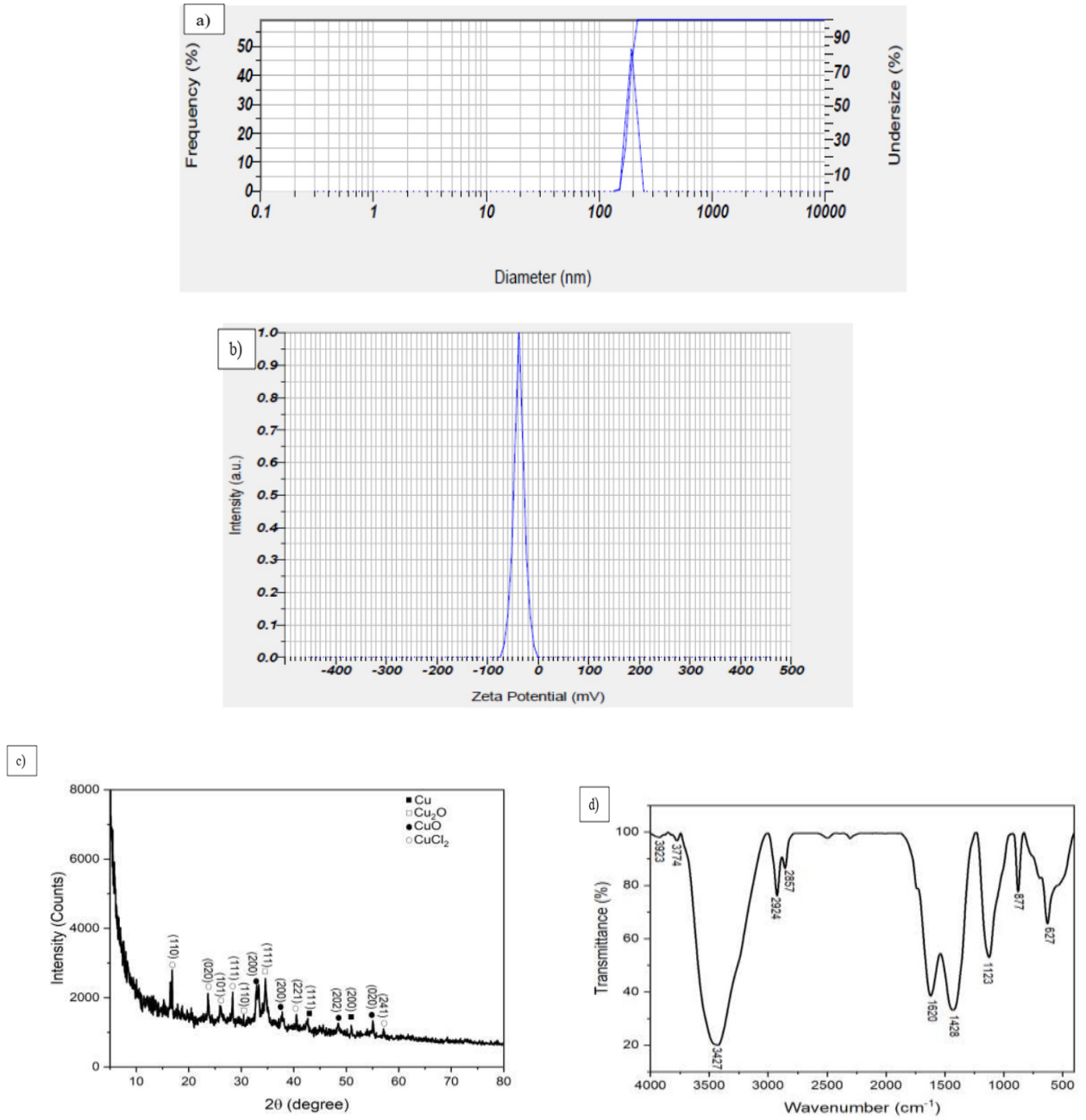

Figure 4) a) Hydrodynamic diameter, (b) zeta potential, and (c) XRD peaks suggest that the crystal structure is somewhat irregular, impurities in the sample are minimal, and distinct peaks are attributed solely to CuNPs. d) FT-IR analysis shows a chemical bond and the specific molecular structure of CuNPs.

sistance, respectively. The same pattern was also observed for the MBCs and sub-MICs of CuNPs, which were between 15.62-125 and 7.8-31.25 µg/mL, respectively (Table 1).

Overall, CuNPs demonstrated more antimicrobial effect against Gram-negative bacteria compared to other groups.

Additionally, the anti-biofilm test results revealed that none of the strains were able to produce biofilm at sub-MICs of CuNPs. Notably, these CuNPs exhibited stronger anti-biofilm activity against Gram-negative *E. coli* and *K. pneumoniae* bacteria, resulting in significantly lower ODs compared to Gram-positive *S. aureus* and *E. faecalis* strains (Figure 5). Finally, CuNPs revealed significant anti-biofilm effects based on the analysis (*: $p<.05$, **: $p<.01$, ***: $p<.001$).

Table 1) MICs, sub-MICs, MBCs, and anti-biofilm properties of CuNPs against bacterial strains

Strain	MICs (µg/mL)	MBCs (µg/mL)	Sub-MICs (µg/mL)
S. aureus	62.5	125	31.25
E. faecalis	31.25	62.5	15.62
E. coli	15.62	31.25	7.8
K. pneumoniae	15.62	15.62	7.8

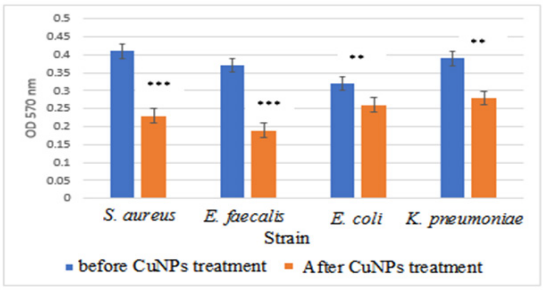

Figure 5) Results of anti-biofilm effects against *E. coli, K. pneumonia, S. aureus*, and *E. faecalis*. *: $p < .05$, **: $p < .01$, ***: $p < .001$.

Discussion

This research evaluated the antimicrobial and anti-biofilm properties of CuNPs produced by green synthesis method using *A. biennis* Willd extract. After synthesis, XRD, DLS, PSD, zeta potential, and FT-IR tests were employed to determine the structure and crystal network of NPs. In the last half-century, CuNPs have been recognized as effective antimicrobial agents, suggesting them as a reservoir for the stable and continuous release of Cu^{+} ions [36]. For the production of different NPs, the green synthesis method is favored because it is more stable, cheaper, effortless, and harmless to humans, animals, and the environment than other chemical methods like vapor deposition, particularly for biomedical applications [37, 38]. In this study, CuNPs synthesis by maceration method was associated with the appearance of brown color from blue, as a result of this color change, CuNPs were identified. Similarly, previous studies have reported the green synthesis of CuNPs from the extract of *A. biennis* Willd [39-41] and other medicinal plants like Cissus arnotiana [42], Capparis zeylanica [43], and Yzygium aromaticum [44].

PSD test was used to check the size and distribution of CuNPs. There is a relationship between the morphology, size, and properties of CuNPs [45]. For example, the frequency of surface plasmon resonance in copper oxide nanoparticles depends on the shape, size, and environmental conditions [46]. Based on PSD analysis, most of the synthesized CuNPs were in the size range of 30 to 40 nm. Because of this ideal size, they were expected to have effective antimicrobial activity against bacteria. The results of DLS also revealed that CuNPs had a suitable diameter, indicating the successful hydrodynamic synthesis of nano-sized particles. In a study by Amjad et al. (2021), UV-Vis (ultraviolet–visible) spectroscopy showed that the average diameter of CuNPs synthesized using Fortunella margarita leaves was within the range of 51.26–56.66 nm [47], which is in agreement with the current and other previous investigations using aqueous sumac [48], Jatropha curcas leaf [49], and Celastrus paniculatus Willd leaf extracts [50].

The zeta potential of NPs provides essential insights into colloid stability. The negative charge acts as a reducing and stabilizing agent that prevents the accumulation of CuNPs. In a study conducted by Karimi et al. (2023), the zeta potential of the synthesized CuNPs was -29.7 mV [40], which is lower than the present study result (-37.8 mV). Sacoto-Figueroa et al. (2021) argued that in therapeutic applications, CuNPs with charges of approximately -30 exhibited significant repulsive force and greater stability in solution [51], which is in agreement with this study findings. According to the literature, CuNPs produced by green synthesis method are considered stable when their zeta potential lies within the range of -30 to +30 mV, including -11 mV [52], –44.3 mV [53], and +25 mV [54].

Other studies have obtained different zeta potentials for NPs, providing critical information about the stability of the formed colloids. The negative charge acts as a reducing and stabilizing agent that prevents the accumulation of CuNPs. The XRD results showed that Cu, CuO, Cu_2O, and $CuCl_2$ were present in the sample with sizes of 5.08, 5.85, 5.22, and 14.4 nm, respectively. The existence of CuNPs was shown by the peak at 2θ values of 35.47°, 38.77°, 48.77°, and 66.21°, and the average crystallite size of CuO calculated by the Debye-Scherrer equation was about 25 nm according to previous studies using *A. biennis* Willd [40]. Also, Suresh et al. (2020) reported that CuO nanostructure prepared using Cynodon dactylon extract indicated diffraction peaks at 2θ values of 32.27°, 35.24°, 38.49°, 48.70°, 53.31°, 57.96°, 61.38°, 66.18°, 67.70°, 72.09°, and 74.94° [31]. The XRD spectrum in the study of Mali and colleagues (2019) showed different distinct diffraction peaks at 37.46°, 50.09°, and 70.48°, which are related to the primary structure of CuO NPs [55] and in agreement with prior research [53, 56].

FTIR spectroscopy could investigate the possible functional groups involved and bond vibrations in the synthesized CuNPs. FT-IR analysis was conducted to determine the potential biomolecules in *A. biennis* Willd extract, which may be involved in the reduction of Cu^+ to CuNPs. In the present study, several peaks were located in the range of 1428 to 3923 cm^{-1} due to the presence of different compound structures. Al-Khafaji and colleagues (2022) [39] highlighted the presence of polyphenols in *A. biennis* Willd extract by FTIR spectroscopy, a spectral band at 1623 cm^{-1} was a hallmark of copper-extract interaction, which is in line with the current study reporting that the peak related to the stretching vibration of Cu-O bonds in CuNPs was located at 627 cm^{-1}. Shanmugapriya et al. (2022) prepared CuNPs using Withania somnifera by green synthesis method, the absorption peak changes of CuNPs at different points were from 561 to 3390 cm^{-1} [57]. In this study, the presence of functional groups such as alkaloids, phenols, halo compounds, and primary and secondary amines was evident in the extract. It is suggested that these functional groups work together to cap and reduce NPs. It has been verified that the produced CuNPs are capped with secondary metabolites of *A. biennis* Willd [58, 59]. The FTIR analysis results in previous similar studies are slightly different from the present study findings regarding the peak values of some compounds, which could be due to the difference in the plants used for the synthesis of CuNPs. Plant extracts have various compounds, which could be different or similar to each other.

The bactericidal and bacteriostatic activities of CuNPs were evaluated in vitro against four bacteria. Based on the results, these effects were more significant on Gram-negative bacteria, indicating that these strains were more sensitive to CuNPs. Generally, *S. aureus* exhibited the highest antimicrobial drug resistance, followed by *E. faecalis, E. coli, and K. pneumonia*, respectively. Gram-positive bacterial cell walls contain thin lipopolysaccharides and thick peptidoglycan layers, which decrease the possibility of CuNPs penetration into bacteria [60]. The results showed that increasing concentrations of CuNPs effectively counteracted the bacterial population, which is consistent with research reporting the antibacterial activity of CuNPs [61, 62]. Different strategies have been proposed by many researchers regarding the antibacterial properties of CuNPs. Leakage of cytoplasmic components, membrane disruption and permeability, and ROS generation are the three most promising mechanisms through which CuNPs inhibit bacterial growth and kill bacteria [63]. Kaviya et al. (2011) [64] argued that CuNPs

had the potential to disrupt/ruin the bacterial cell membrane, resulting in bacterial lysis. Another study reported the release and accumulation of Cu^{+} ions in lipopolysaccharide and membrane protein channels as two important mechanisms employed by CuNPs to lyse bacteria [65].

In the continuation of the investigation, none of the studied bacteria formed biofilms in the presence of sub-MICs of CuNPs. It was evident that CuNPs had more anti-biofilm effects on Gram-negative than Gram-positive bacteria due to lower ODs. Similarly, some studies have shown the anti-biofilm properties of CuNPs against Streptococcus mutans [66], *Pseudomonas*, and *Listeria monocytogenes* [67] as well as *S. aureus, P. fluorescens*, *L. monocytogenes, Fusarium moniliforme,* and *Aspergillus niger* [53]. Biofilm formation is of great importance in the food industry and the treatment of many infectious diseases, and it seems that NPs have been successful in preventing biofilm production, even the Food and Drug Administration (FDA) has permitted the use of metallic NPs in food packaging materials. [14]. Recent studies have indicated that anti-quorum sensing strategies that inhibit signaling pathways, such as limiting N-acyl homo-serine lactones (AHLs), could reduce bacterial population density, disrupt bacterial motility, and ultimately eliminate biofilm [68].

Conclusion

Based on the findings, it could be concluded that *A. biennis* Willd could be applied as a proper alternative in the green synthesis of CuNPs due to their physical characteristics. The green production method is considered as a clean, cost-effective, low-risk, and environmentally friendly method. CuNPs showed antibacterial activities through growth inhibition and were more effective against Gram-negative strains owing to lower MICs, sub-MICs, and MBCs. This study suggests the use of CuNPs as an adjunctive therapeutic agent in the treatment of infectious diseases.

Acknowledgments

The authors would like to acknowledge the staff of the Department of Microbiology, Shahr-e-Qods Branch, Islamic Azad University (IAU), Tehran, Iran.

Ethical approval: The present research was conducted using a standard bacterial strain under the ethical approval of the Department of Microbiology, Shahr-e-Qods Branch, Islamic Azad University, Tehran, Iran. The study was part of a student thesis, and all ethical guidelines were strictly adhered to, with full authorization from the university to conduct this research.

Authors' contributions: SF and FR; Data curation and formal analysis: SF and AF; Validation: SF, FR; Investigation and writing of the original draft: SF and AF; supervision: FR. All authors reviewed and approved the final manuscript.

Conflicts of interests: None declared by authors.

Fundings: None declared by authors.

Consent to participate: Not applicable.

References

1. Sabzi S, Shahbazi S, Noori Goodarzi N, Haririzadeh Jouriani F, Habibi M, Bolourchi N, et al. Genome-wide subtraction analysis and reverse vaccinology to detect novel drug targets and potential vaccine candidates against ehrlichia chaffeensis. Appl Biochem Biotechnol. 2023;195(1):107-24.
2. Shahbazi S, Sabzi S, Goodarzi NN, Fereshteh S, Bolourchi N, Mirzaie B, et al. Identification of novel putative immunogenic targets and construction of a multi-epitope vaccine against multidrug-resistant Corynebacterium jeikeium using reverse vaccinology approach. Microb Pathog. 2022;164:105425.
3. Shahkolahi S, Shakibnia P, Shahbazi S, Sabzi S, Badmasti F, Asadi Karam MR, et al. Detection of ESBL and AmpC producing Klebsiella pneumoniae ST11 and ST147 from urinary tract infections in Iran. Acta Microbiol Immunol Hung.

2022;69(4):303-13.
4. Taati Moghadam M, Hossieni Nave H, Mohebi S, Norouzi A. The evaluation of connection between integrons class I and II and ESBL-producing and non-ESBL Klebsiella pneumoniae isolated from clinical samples, Kerman. Iran J Med Microbiol. 2016;10(4):1-9.
5. Lewis K. New approaches to antimicrobial discovery. Biochem Pharmacol. 2017;134:87-98.
6. Rahmati F. Identification and characterization of Lactococcus starter strains in milk-based traditional fermented products in the region of Iran. AIMS Agric Food. 2018;3(1):12-25.
7. Magalhães C, Lima M, Trieu-Cuot P, Ferreira P. To give or not to give antibiotics is not the only question. Lancet Infect Dis. 2021;21(7):e191-201.
8. Shahbazi S, Badmasti F, Habibi M, Sabzi S, Noori Goodarzi N, Farokhi M, et al. In silico and in vivo investigations of the immunoreactivity of Klebsiella pneumoniae OmpA protein as a vaccine candidate. Iran Biomed J. 2024;28(4):156-67.
9. Reygaert WC. An overview of the antimicrobial resistance mechanisms of bacteria. AIMS Microbiol. 2018;4(3):482-501.
10. Rahmati F. Characterization of Lactobacillus, Bacillus, and Saccharomyces isolated from Iranian traditional dairy products for potential sources of starter cultures. AIMS Microbiol. 2017;3(4):815-25.
11. Shahbazi S, Shivaee A, Nasiri M, Mirshekar M, Sabzi S, Sariani OK. Zinc oxide nanoparticles impact the expression of the genes involved in toxin–antitoxin systems in multidrug-resistant Acinetobacter baumannii. J Basic Microbiol. 2023;63(9):1007-15.
12. Shivaee A, Meskini M, Shahbazi S, Zargar M. Prevalence of flmA, flmH, mrkA, ecpA, and mrkD virulence genes affecting biofilm formation in clinical isolates of K. pneumonia. Feyz Med Sci J. 2019;23(2):168-76.
13. Moghadam MT, Chegini Z, Khoshbayan A, Farahani I, Shariati A. Helicobacter pylori biofilm and new strategies to combat it. Curr Mol Med. 2021;21(7):549-61.
14. Rahmati F, Hosseini SS, Mahuti Safai S, Asgari Lajayer B, Hatami M. New insights into the role of nanotechnology in microbial food safety. 3 Biotech. 2020;10:1-15.
15. Ruhal R, Kataria R. Biofilm patterns in Gram-positive and Gram-negative bacteria. Microbiol Res. 2021;251:126829.
16. Rahmati F. Microencapsulation of Lactobacillus acidophilus and Lactobacillus plantarum in Eudragit S100 and alginate chitosan under gastrointestinal and normal conditions. Appl Nanosci. 2020;10(2):391-9.
17. Shahbazi S, Habibi M, Badmasti F, Sabzi S, Farokhi M, Karam MR. Design and fabrication of a vaccine candidate based on rOmpA from Klebsiella pneumoniae encapsulated in silk fibroin-sodium alginate nanoparticles against pneumonia infection. Int Immunopharmacol. 2023;125:111171.
18. Sabzi S, Habibi M, Badmasti F, Shahbazi S, Karam MR, Farokhi M. Polydopamine-based nano adjuvant as a promising vaccine carrier induces significant immune responses against Acinetobacter baumannii-associated pneumonia. Int J Pharm. 2024;654:123961.
19. Parvaei M, Habibi M, Shahbazi S, Babaluei M, Farokhi M, Karam MR. Immunostimulatory chimeric protein encapsulated in gelatin nanoparticles elicits protective immunity against Pseudomonas aeruginosa respiratory tract infection. Int J Biol Macromol. 2024;277:133964.
20. Rahmati F. Impact of microencapsulation on two probiotic strains in alginate chitosan and Eudragit S100 under gastrointestinal and normal conditions. Open Biotechnol J. 2019;13(1):59-67.
21. Jayarambabu N, Akshaykranth A, Rao TV, Rao KV, Kumar RR. Green synthesis of Cu nanoparticles using Curcuma longa extract and their application in antimicrobial activity. Mater Lett. 2020;259:126813.
22. Wang C, Liu Y, Cui Z, Yu X, Zhang X, Li Y, et al. In situ synthesis of Cu nanoparticles on carbon for highly selective hydrogenation of furfural to furfuryl alcohol by using pomelo peel as the carbon source. ACS Sustain Chem Eng. 2020;8(34):12944-55.
23. Zhou X, Shen B, Zhai J, Hedin N. Reactive oxygenated species generated on iodide-doped BiVO4/BaTiO3 heterostructures with Ag/Cu nanoparticles by coupled piezophototronic effect and plasmonic excitation. Adv Funct Mater. 2021;31(13):2009594.
24. Fan X, Yahia LH, Sacher E. Antimicrobial properties of the Ag, Cu nanoparticle system. Biology. 2021;10(2):137.
25. Ameen F. Optimization of the synthesis of fungus-mediated bi-metallic Ag-Cu nanoparticles. Appl Sci. 2022;12(3):1384.
26. Ying S, Guan Z, Ofoegbu PC, Clubb P, Rico C, He F, et al. Green synthesis of nanoparticles: Current developments and limitations. Environ Technol Innov. 2022;26:102336.
27. Hussain M, Thakur RK, Khazir J, Ahmed S, Khan MI, Rahi P, et al. Traditional uses, phytochemistry, pharmacology, and toxicology of the genus Artemisia L.(Asteraceae): A high-value medicinal plant. Curr Top Med Chem. 2024;24(4):301-42.
28. Sancar PY, Tukur U, Civelek S, Kursat M. The molecular investigations on the subgenus

Artemisia Less. of the genus Artemisia L.(Asteraceae) in Turkey. Braz J Biol. 2021;83:e252656.
29. Tambun R, Alexander V, Ginting Y. Performance comparison of maceration method, soxhletation method, and microwave-assisted extraction in extracting active compounds from soursop leaves (Annona muricata): A review. IOP Conf Ser Mater Sci Eng. 2021;1122(1):01209530. de Sousa ES, Cortez AC, de Souza Carvalho Melhem M, Frickmann H, de Souza JV. Factors influencing susceptibility testing of antifungal drugs: A critical review of document M27-A4 from the Clinical and Laboratory Standards Institute (CLSI). Braz J Microbiol. 2020;51:1791-800.
31. Suresh S, Ilakiya R, Kalaiyan G, Thambidurai S, Kannan P, Prabu K, et al. Green synthesis of copper oxide nanostructures using Cynodon dactylon and Cyperus rotundus grass extracts for antibacterial applications. Ceram Int. 2020;46(8):12525-37.
32. El-Seedi HR, El-Shabasy RM, Khalifa SA, Saeed A, Shah A, Shah R, et al. Metal nanoparticles fabricated by green chemistry using natural extracts: Biosynthesis, mechanisms, and applications. RSC Adv. 2019;9(42):24539-59.
33. Yadav S, Nadar T, Lakkakula J, Wagh NS. Biogenic synthesis of nanomaterials: Bioactive compounds as reducing and capping agents. In: Biogenic nanomaterials for environmental sustainability: Principles, practices, and opportunities. Switzerland, Cham: Springer International Publishing; 2024, p. 147-88.
34. Vijayaraghavan K, Ashokkumar T. Plant-mediated biosynthesis of metallic nanoparticles: A review of literature, factors affecting synthesis, characterization techniques, and applications. J Environ Chem Eng. 2017;5(5):4866-83.
35. Gulati S, Sachdeva M, Bhasin K. Capping agents in nanoparticle synthesis: Surfactant and solvent system. AIP Conf Proc. 2018;1953(1):030214.
36. El-Rab SM, Basha S, Ashour AA, Enan ET, Alyamani AA, Felemban NH. Green synthesis of copper nano-drug and its dental application upon periodontal disease-causing microorganisms. J Microbiol Biotechnol. 2021;31(12):1656-66.
37. Ijaz I, Gilani E, Nazir A, Bukhari A. Detail review on chemical, physical, and green synthesis, classification, characterizations, and applications of nanoparticles. Green Chem Lett Rev. 2020;13(3):223-45.
38. Dikshit PK, Kumar J, Das AK, Sadhu S, Sharma S, Singh S, et al. Green synthesis of metallic nanoparticles: Applications and limitations. Catalysts. 2021;11(8):902.
39. Al-Khafaji MA, Al-Refai'a RA, Al-Zamely OM. Green synthesis of copper nanoparticles using Artemisia plant extract. Mater Today Proc. 2022;49:2831-5.
40. Karimi B, Mardani M, Kaboutari J, Javdani M, Albadi J, Shirian S. Green synthesis of copper nanoparticles using Artemisia annua aqueous extract and its characterization, antioxidant and burn wound healing activities. Chem Pap. 2024;78:231-43.
41. Hayat K, Ali S, Ullah S, Fu Y, Hussain M. Green synthesized silver and copper nanoparticles induced changes in biomass parameters, secondary metabolites production, and antioxidant activity in callus cultures of Artemisia absinthium L. Green Process Synth. 2021;10(1):61-72.
42. Rajeshkumar S, Menon S, Kumar SV, Tambuwala MM, Bakshi HA, Mehta M, et al. Antibacterial and antioxidant potential of biosynthesized copper nanoparticles mediated through Cissus arnotiana plant extract. J Photochem Photobiol B. 2019;197:111531.
43. Saranyaadevi K, Subha V, Ravindran R, Renganathan S. Synthesis and characterization of copper nanoparticle using Capparis zeylanica leaf extract. Int J Chem Tech Res. 2014;6(10):4533-41.
44. Rajesh K, Ajitha B, Reddy YA, Suneetha Y, Reddy PS. Assisted green synthesis of copper nanoparticles using Syzygium aromaticum bud extract: Physical, optical, and antimicrobial properties. Optik. 2018;154:593-600.
45. Valdez-Salas B, Beltrán-Partida E, Zlatev R, Stoytcheva M, Gonzalez-Mendoza D, Salvador-Carlos J, et al. Structure-activity relationship of diameter controlled Ag@ Cu nanoparticles in broad-spectrum antibacterial mechanism. Mater Sci Eng C. 2021;119:111501.
46. Barchiesi D, Gharbi T, Cakir D, Anglaret E, Fréty N, Kessentini S, et al. Performance of surface plasmon resonance sensors using copper/copper oxide films: Influence of thicknesses and optical properties. Photonics. 2022;9(2):104.
47. Amjad R, Mubeen B, Ali SS, Imam SS, Alshehri S, Ghoneim MM, et al. Green synthesis and characterization of copper nanoparticles using Fortunella margarita leaves. Polymers. 2021;13(24):4364.
48. Ismail M. Green synthesis and characterizations of copper nanoparticles. Mater Chem Phys. 2020;240:122283.
49. Ghosh MK, Sahu S, Gupta I, Ghorai TK. Green synthesis of copper nanoparticles from an extract of Jatropha curcas leaves: Characterization, optical properties, CT-DNA binding, and photocatalytic activity. RSC Adv. 2020;10(37):22027-35.
50. Mali SC, Dhaka A, Githala CK, Trivedi R. Green synthesis of copper nanoparticles using

Celastrus paniculatus Willd leaf extract and their photocatalytic and antifungal properties. Biotechnol Rep. 2020;27:e00518.
51. Sacoto-Figueroa FK, Bello-Toledo HM, González-Rocha GE, Luengo Machuca L, Lima CA, Meléndrez-Castro M, et al. Molecular characterization and antibacterial activity of oral antibiotics and copper nanoparticles against endodontic pathogens commonly related to health care-associated infections. Clin Oral Investig. 2021;25(12):6729-41.
52. Ullah H, Wilfred CD, Shaharun MS. Green synthesis of copper nanoparticle using ionic liquid-based extraction from Polygonum minus and their applications. Environ Technol. 2019;40(28):3705-12..
53. Pandit R, Gaikwad S, Rai M. Biogenic fabrication of CuNPs, Cu bioconjugates, and in vitro assessment of antimicrobial and antioxidant activity. IET Nanobiotechnol. 2017;11(5):568-75.
54. Müller E, Behra R, Sigg L. Toxicity of engineered copper (Cu0) nanoparticles to the green alga Chlamydomonas reinhardtii. Environ Chem. 2015;13(3):457-63.
55. Mali SC, Raj S, Trivedi R. Biosynthesis of copper oxide nanoparticles using Enicostemma axillare (Lam.) leaf extract. Biochem Biophys Rep. 2019;20:100699.
56. Shende S, Ingle AP, Gade A, Rai M. Green synthesis of copper nanoparticles by Citrus medica Linn. (Idilimbu) juice and its antimicrobial activity. World J Microbiol Biotechnol. 2015;31:865-73.
57. Shanmugapriya J, Reshma C, Srinidhi V, Harithpriya K, Ramkumar K, Umpathy D, et al. Green synthesis of copper nanoparticles using Withania somnifera and its antioxidant and antibacterial activity. J Nanomater. 2022;2022(1):7967294.
58. Ahmad T, Irfan M, Bustam MA, Bhattacharjee S. Effect of reaction time on green synthesis of gold nanoparticles by using aqueous extract of Elaise guineensis (oil palm leaves). Procedia Eng. 2016;148:467-72.
59. Bhavyasree P, Xavier T. Green synthesised copper and copper oxide based nanomaterials using plant extracts and their application in antimicrobial activity. Curr Res Green Sustain Chem. 2022;5:100249.
60. Khorsandi K, Keyvani-Ghamsari S, Khatibi Shahidi F, Hosseinzadeh R, Kanwal S. A mechanistic perspective on targeting bacterial drug resistance with nanoparticles. J Drug Target. 2021;29(9):941-59.
61. Govarthanan M, Cho M, Park JH, Jang JS, Yi YJ, Kamala-Kannan S, et al. Cottonseed oilcake extract mediated green synthesis of silver nanoparticles and its antibacterial and cytotoxic activity. J Nanomater. 2016;2016(1):7412431.
62. Kumar PV, Shameem U, Kollu P, Kalyani R, Pammi S. Green synthesis of copper oxide nanoparticles using Aloe vera leaf extract and its antibacterial activity against fish bacterial pathogens. Bionanoscience. 2015;5:135-9.
63. Nisar P, Ali N, Rahman L, Ali M, Shinwari ZK. Antimicrobial activities of biologically synthesized metal nanoparticles: An insight into the mechanism of action. J Biol Inorg Chem. 2019;24:929-41.
64. Kaviya S, Santhanalakshmi J, Viswanathan B, Muthumary J, Srinivasan K. Biosynthesis of silver nanoparticles using Citrus sinensis peel extract and its antibacterial activity. Spectrochim Acta A Mol Biomol Spectrosc. 2011;79(3):594-8.
65. Tovar-Corona A, Lobo-Sánchez M, Herrera-Perez J, Zanella R, Rodriguez-Mora J, Vázquez-Cuchillo O. Green synthesis of copper (0) nanoparticles with cyanidine-O-3-glucoside and its strong antimicrobial activity. Mater Lett. 2018;211:266-9.
66. Eshed M, Lellouche J, Gedanken A, Banin E. A Zn-doped CuO nanocomposite shows enhanced antibiofilm and antibacterial activities against Streptococcus mutans compared to nanosized CuO. Adv Funct Mater. 2014;24(10):1382-90.
67. Ghasemian E, Naghoni A, Rahvar H, Kialha M, Tabaraie B. Evaluating the effect of copper nanoparticles in inhibiting Pseudomonas aeruginosa and Listeria monocytogenes biofilm formation. Jundishapur J Microbiol. 2015;8(5):e17430.
68. Shamshad S, Rajagopal S. Current trends and advances of quorum sensing inhibitors and their biotechnological applications. Indian J Biochem Biophys. 2023;60(4):255-80.